JOURNAL OF MATERIALS SCIENCE 15 (1980) 987–996

Crack blunting mechanisms in polymers

A. J. KINLOCH
Ministry of Defence (P.E.), Propellants Explosives and Rocket Motor Establishment, Waltham Abbey, Essex, UK

J. G. WILLIAMS
Department of Mechanical Engineering, Imperial College of Science and Technology, London SW7 2BX, UK

A quantitative model has been developed to account for the degree of blunting that occurs at crack tips in epoxy materials prior to the onset of crack propagation. This mechanism controls the subsequent mode of crack growth and, to a large extent, the toughness as defined by the stress intensity factor for crack initiation. From this model a unique fracture criterion is derived which is applicable over all modes of crack propagation.

1. Introduction

Epoxy resins are widely employed as the basis for adhesive compositions and as the matrix material for glass-, polyamide- and carbon-fibre composites and are, therefore, being increasingly used in structural engineering applications. This has led to interest being focussed on identifying mechanisms and criteria of crack initiation and propagation in epoxy resin materials and, since they are usually brittle and general yielding does not occur, a linear elastic fracture mechanics approach has frequently been adopted [1, 2].

However, the detailed interpretation of their fracture behaviour has been inhibited by the complex crack growth modes reported in the literature but recent work [3, 4] has established the following pattern in their brittle fracture behaviour.

(1) Crack growth may occur at a constant load with the rate of crack propagation being dependent upon the rate of cross-head displacement employed. This is termed "stable" crack growth and a typical load–displacement trace for a specimen exhibiting this type of behaviour is shown in Fig. 1a. This mode of crack growth is generally favoured by using relatively fast displacement rates or low test temperatures and, under such conditions the stress intensity factor, K_I, (or fracture energy) required for crack initiation is comparatively low and almost independent of test temperature and rate.

(2) Alternatively, crack propagation may occur intermittently in a stick–slip manner exhibiting load values appropriate to both crack initiation and crack arrest. This is termed "unstable" crack growth and a typical load–displacement trace is shown in Fig. 1b. This mode of growth is favoured at relatively slow displacement rates or high test temperatures. The stress intensity factor for crack initiation is usually rate/temperature dependent and greater than the value for crack arrest which is virtually rate/temperature independent. Further, if a transition from unstable to stable crack growth can be induced in the material, for example by lowering the test temperature, it is found that the stress intensity factor for crack arrest (unstable crack growth behaviour) has approximately the same value as that for stable crack growth.

Apart from test temperature and rate, other parameters that have been shown to affect the type of crack growth behaviour including curing agent [5–7], cure schedule [5, 8, 9], filler content [10] and environment [6, 11].

Now a mechanism has recently been proposed which explains qualitatively the above observations [3, 4]. Essentially it proposes that the amount of localized plastic deformation that occurs at the crack tip prior to crack propagation is the controlling feature and thus emphasises the role of crack tip blunting. The evidence for this mechanism is first, when continuous crack propagation

0022–2461/80/040987–10$03.00/0

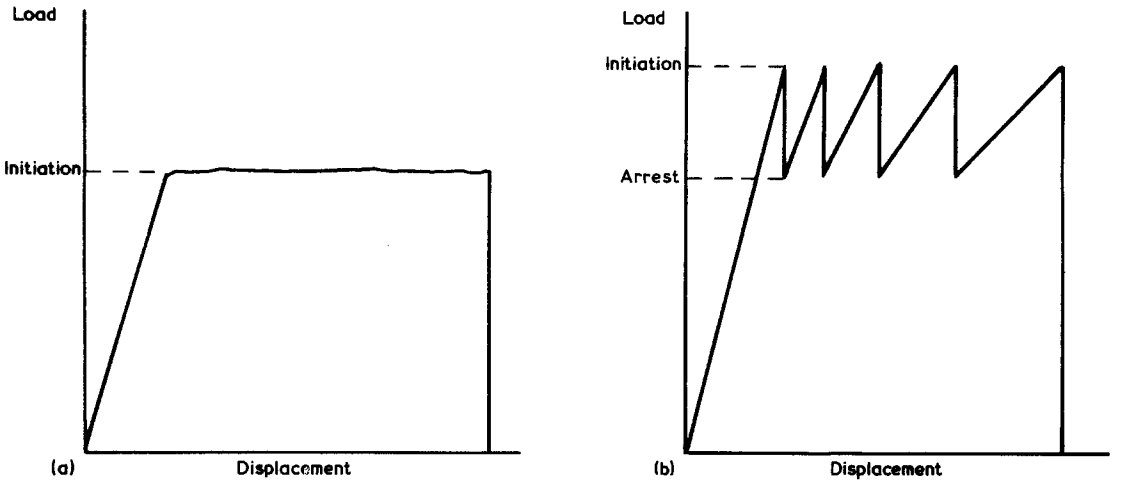

Figure 1 Typical load–displacement curves for (a) stable, continuous crack propagation; (b) unstable, stick–slip crack propagation.

occurs a constant crack-opening displacement at the crack tip provides a unique failure criterion while the value of this parameter rises rapidly when the material undergoes a transition from stable to stick–slip propagation. This was interpreted as a clear indication that blunting of the crack tip had taken place when stick–slip propagation resulted. Second, the yield stresses of the epoxy materials decrease as the strain rate is reduced or the temperature raised. This implies that plastic deformation ahead of the crack tip should be easier under those conditions, which are the very ones which favour stick–slip crack propagation. If the degree of plastic deformation is high the crack tip will be severely blunted and hence, when the crack eventually propagates, the rate of release of energy will be greater than that required for a stable crack, so the crack will rapidly accelerate and unstable crack growth results; i.e. K_I (onset crack propagation) $> K_I$ (stable crack propagation). Third, this qualitative argument may also be readily employed to explain the increase in toughness and the change from stable to unstable crack growth that has been observed in some epoxy resins after having been subjected to a constant load just below the short-term fracture load for a few days prior to testing [12] or by exposing the material to high humidity or water for a short period prior to testing [6, 11]. These conditions would be predicted to increase the ability of the material to undergo greater deformation in the vicinity of the crack tip; due to the lower strain rate or to local plasticization respectively.

This paper extends this approach by examining the crack propagation data for a wide range of epoxy materials, including rubber-toughened resins, obtained from different test conditions and directly correlates this data with the yield behaviour of the material. A quantitative model is then developed for the degree of crack tip blunting incurred at the crack tip and this enables all the fracture data to be unified and a general failure criterion to be established.

2. Experimental

2.1. Materials

The resin employed was a commercial diglycidyl ether of bisphenol A (DGEBA) epoxy resin and the various curing agents and cure schedules used are shown in Table I.

2.2. Crack propagation

Most of the crack propagation data has been previously reported [3, 6], so only the essential features need to be highlighted. The epoxy resin materials were either tested in the form of bulk material, when a double torsion [3] or a compact tension [13] geometry was employed, or as an adhesive when a tapered double cantilever beam joint [3, 4] was used. Previous work [3] has shown that crack propagation in the adhesive joints is completely analogous to that in the bulk material when simple epoxy materials are involved and centre-of-bond failure occurs, as were the conditions in the above work. In all cases the appropriate values of the stress intensity factor, K_I, were determined.

2.3. Yield behaviour

Since all the materials studied fracture when

TABLE I Formulations and cure schedules for epoxy materials

Epoxy resin	Curing agent	Parts per hundred of resin used	Cure schedule
DGEBA	Triethylenetetramine (TETA)	9.8	23 h/23° C + 3 h/100° C
DGEBA	Tetraethylenepentamine (TEPA)	10.0	22 h/23° C + 6 h/80° C
DGEBA	Tri-2-ethylhexanoate of 2, 4, 6-tris(dimethylaminomethyl phenol) (a 3° amine)	9.4	96 h/23° C + $1\frac{1}{4}$ h/100° C + $2\frac{1}{2}$ h/180° C
DGEBA	Piperidine	5.0	16 h/120° C
DGEBA resin + 10 phr CTBN (a) (Rubber-modified epoxy)	Piperidine	5.0	16 h/120° C

(a) Carboxyl-terminated butadiene-acrylonitrile rubber.

tested in uniaxial tension prior to yielding, their yield behaviour was examined by testing in uniaxial compression. They were cast and machined into cylindrical blocks with a height to diameter ratio of about 2 to 1. The blocks were deformed in a compression cage between polished steel plates, lubricated and molybdenum disulphide grease, in an Instron mechanical testing machine. A constant cross-head displacement rate, $\dot{y}$, was used for each test and this was converted to a strain rate using the specimen dimensions. The nominal strain, e, was determined from the cross-head displacement corrected for the machine deflection using a steel blank. The load, P, was measured from the Instron chart and converted into a true stress, σ_y, using the initial specimen cross-sectioned area, A_0, in the equation:

$$\sigma_y = \frac{P}{A_0}(1 - e) \quad (1)$$

which assumes constant volume deformation.

3. Results and discussion

3.1. Effect of displacement rate

The effect of displacement rate, $\dot{y}$, on the fracture behaviour of four epoxy resin materials tested at 22° C is shown in Table II. In the present paper K_{IB} has been defined as the measured stress intensity factor for the onset of crack growth and K_{Ic} as the minimum value of the stress intensity factor required for crack propagation in the given material, i.e. K_{Ic} represents the value that is

TABLE II Effect of varying displacement rate using different epoxy materials (test temperature 22 ± 2° C)

$\text{Log}_{10}\dot{y}$ (m sec^{-1})	Type of crack growth	K_{IB}/K_{Ic}	σ_y (MPa)	e_y	δ_t (μm)
DGEBA/10 phr TEPA					
−5.67	Stable	0.93	111	0.05	0.65
−4.67	Stable	0.98	116	0.055	0.72
−4.37	Stable	1.00	117	0.055	0.74
−3.37	Stable	1.02	121	0.060	0.79
−2.37	Stable	1.03	126	0.060	0.83
DGEBA/9.8 phr TETA					
−6.07	Unstable	1.25	101	0.045	2.82
−4.67	Stable	0.98	108	0.055	1.81
−4.07	Stable	1.00	118	0.065	1.91
−2.67	Stable	0.94	120	0.065	1.80
DGEBA/3° amine					
−6.07	Unstable	2.00	72	0.05	12.10
−4.07	Unstable	1.41	83	0.065	5.88
−2.07	Unstable	1.10	98	0.08	3.16

Values of K_{Ic}: DGEBA/10 phr TEPA, 0.43 MN m$^{-3/2}$; DGEBA/9.8 phr TETA, 0.64 MN m$^{-3/2}$; DGEBA/3° amine, 0.56 MN m$^{-3/2}$.

TABLE III Effect of temperature using different epoxy materials

Temperature (° C)	$\text{Log}_{10}\dot{y}$ (m sec^{-1})	Type of crack growth	K_{IB}/K_{Ic}	σ_y (MPa)	e_y	δ_t (μm)
DGEBA/9.8 phr TETA						
+ 67	−4.37	Unstable	1.90	75	0.06	15.77
+ 45	−4.37	Unstable	1.20	96	0.08	5.12
−40	−4.37	Stable	1.03	160	0.10	1.75
Rubber-modified epoxy			(b)			
+ 60	−5.00	(a)	2.72	42	0.05	537
+ 60	−4.37	(a)	2.31	45	0.05	337
+ 22	−4.37	Unstable	1.47	70	0.055	62.1
+ 22	−3.37	Unstable	1.31	80	0.055	37.8
−20	−4.37	Unstable	1.06	90	0.06	21.3
−60	−4.37	Stable	1.00	110	0.065	12.6

(a) Gross shear-yielding stabilized crack propagation.
(b) K_{Ic} for rubber-modified epoxy, 1.60 MN m$^{-3/2}$.

obtained when the material contains a sharp crack while K_{IB} the value which results from the crack having blunted during the test. For brittle, stable crack growth K_{IB} and K_{Ic} have within experimental error the same value so $K_{IB}/K_{Ic} \approx 1$. For unstable crack propagation K_{IB} represents the initiation value while K_{Ic} has been taken as the arrest value; the arrest value from unstable cracking being approximately equivalent to the initiation value for stable crack growth [3, 6, 14].

Also shown in Table II are the true compressive yield stress, σ_y, and the yield strain, e_y.

Now, as may be seen, unstable crack growth, and hence values of $K_{IB}/K_{Ic} > 1$, were dominant for the DGEBA/3° amine and, at low displacement rates, for the DGEBA/9.8 TETA material. Examination of the respective yield behaviour reveals that these conditions were exactly those where relatively low yield stresses were recorded, typically below about 100 MPa. On the other hand the epoxy material which always exhibited stable crack growth, i.e. DGEBA/10 phr* TEPA, possessed higher values of yield stress over the complete range of displacement rates.

3.2. Effect of temperature

The effect of temperature on the K_{IB}/K_{Ic} ratio and the yield stress value for the DGEBA/9.8 phr TETA material is shown in Table III and dramatically illustrates the inverse correlation between yield stress and K_{IB}/K_{Ic} ratio.

Also shown in Table III are results from crack propagation studies on a rubber-toughened epoxy, measured using a compact tension testpiece [13]. At 22° C the yield stresses are comparatively low, the K_{IB}/K_{Ic} values are greater than unity and unstable crack growth occurs. However, at 60° C a further complexity in the crack growth behaviour occurs compared to the data from the simple epoxies. Low yield stress values ($\sigma_y \leqslant 45$ MPa) are recorded but stable, rather than unstable, crack growth is observed. The appearance of the fracture surfaces immediately provided the reason for this apparent contradiction. Unlike the stable crack growth which has been observed in the simple epoxies, where the fracture surface was almost featureless apart from a few minor river markings, for the rubber toughened epoxies at 60° C the surfaces revealed that a highly ductile fracture had occurred and was even accompanied by the presence of shear lips. Thus crack propagation had occurred by a tearing mode and, as would be expected, required a high value of K_{IB} (again in contrast to the simple epoxy resins where stable, brittle crack growth occurs at a comparatively very low value of K_{Ic}). This mechanism has undoubtedly been responsible for similar results reported recently [15]. Taking the value of K_{Ic} for the rubber toughened epoxy material to be the arrest value at 22° C (i.e. 1.6 MN m$^{-3/2}$, with the arrest value being largely insensitive to temperature) then the strong inverse correlation between the K_{IB}/K_{Ic} ratio and σ_y is again clearly evident.

3.3. Effect of time under constant load

Recent work has shown that epoxy resins, both in the bulk [16] and in joints [12] do not always show static fatigue failure. Some resins, especially

*phr = per hundred parts resin.

TABLE IV Effect of time under constant load (test temperature 22 ± 2° C; $\dot{y} = 8.3 \times 10^{-6}$ m sec^{-1})

$\text{Log}_{10}\ t$ (sec)	Type of crack growth	K_{IB}/K_{Ic}	σ_y (MPa)	e_y	δ_t (μm)
DGEBA/10 phr TEPA					
1.00	Stable	1	120	0.06	0.77
2.28	Stable	1	116	0.055	0.76
2.70	Unstable	1.06	114	0.055	0.88
3.02	Unstable	1.03	112	0.05	0.78
4.26	Unstable	1.22	106	0.05	1.22
6.08	Unstable	1.35	98	0.045	1.58
6.35	Unstable	1.40	96	0.045	1.77
7.71	Unstable	1.43	95	0.04	1.68

those which usually exhibit continuous crack propagation behaviour in constant $\dot{y}$ tests, do not appear to suffer from time dependent failure during a reasonable timescale even when loaded to about 90 to 95% of the short term stress intensity factor, K_{Ic}. It has been further shown [12] that if the static fatigue test of such a material is interrupted and a constant $\dot{y}$ test performed, the epoxy resin generally shows stick–slip crack propagation rather than continuous propagation for the initial crack movement. This occurs at a much higher value of K_I than for the continuous propagation observed in the material before being subjected to static loading. However, after the first jump, propagation takes place in a continuous manner at the original value of the stress intensity factor, K_{Ic}.

Table IV shows the constant displacement rate fracture results after subjecting the specimen to various time periods under a constant load; the K_{IB}/K_{Ic} ratios refer to the first increment of crack growth and are taken from the work of Gledhill *et al.* [12] where a DGEBA/10 phr TEPA material was studied. The corresponding values of σ_y and e_y are also given and it is of interest to note that the true compressive yield stress, σ_y, decreases with increasing time of test [3]. Thus, the formation of a plastic-zone at the crack tip should be easier at longer times and hence the degree of crack blunting will increase. It is suggested that it is an increase in the severity of crack tip blunting that is responsible for the rise in K_{IB} and associated change in crack propagation behaviour from stable to unstable upon re-testing at a constant $\dot{y}$. However, once the crack has propagated through the blunting region further propagation occurs in a stable manner at the original K_I value, i.e. at K_{Ic}. This tendency for the crack to blunt under static fatigue conditions means that although the applied load may initially represent a large percentage of that required for fracture this rapidly diminishes as the static fatigue test proceeds. Thus the self-toughening mechanism forestalls static fatigue failure.

3.4. Correlation between K_{IB}/K_{Ic} ratio and yield stress

The correlation between increasing K_{IB}/K_{Ic} ratio and decreasing yield stress has been discussed above for each epoxy material and test condition employed. However, it is of particular interest to note that a master curve exists between K_{IB}/K_{Ic} and σ_y, as shown in Fig. 2. Further, the type of crack growth may also be directly related to the values of these parameters.

4. Crack blunting mechanisms

4.1. Theoretical

From the above discussions, it appears that the yield behaviour of the material in the vicinity of the crack tip controls the degree of plastic deformation that occurs locally and hence the measured toughness and mode of crack growth. This naturally leads to a consideration of the stress distribution around a blunt crack. It has been shown [2] that for a crack of tip radius, ρ, and length, a, then the stress, σ_{yy}, normal to the axis of the crack at a small distance, r, ahead of the tip (Fig. 3) is given by

$$\sigma_{yy} = \frac{\sigma_0\sqrt{a}}{\sqrt{(2r)}} \frac{(1 + \rho/r)}{(1 + \rho/2r)^{3/2}} \qquad (2)$$

where σ_0 is the applied stress. Now, if it is postulated that fracture occurs when a critical stress, σ_c, is attained at a certain distance, c, ahead of the crack tip, then $\sigma_{yy} = \sigma_c$ and $r = c$, and Equation 2 becomes

$$\sigma_c = \frac{\sigma_0\sqrt{a}}{\sqrt{(2c)}} \frac{(1 + \rho/c)}{(1 + \rho/2c)^{3/2}}. \qquad (3)$$

The measured stress intensity factor, K_{IB}, at the onset of crack growth is related to the applied

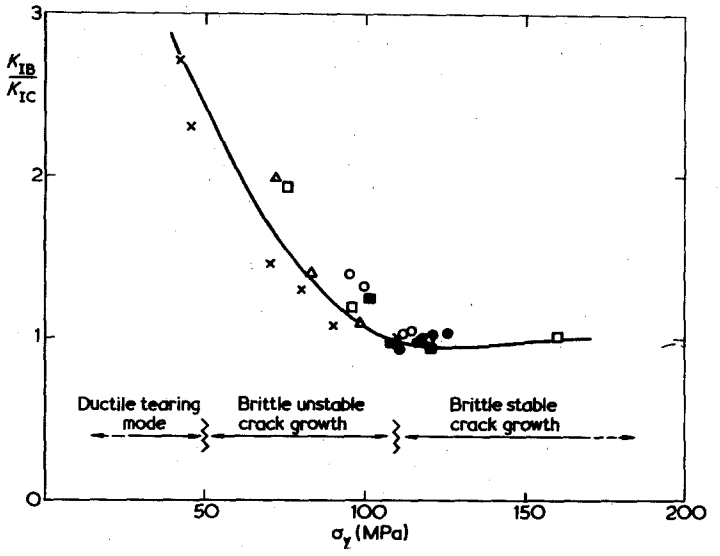

Figure 2 Relation between K_{IB}/K_{Ic} ratio, yield stress and crack growth mode. □ DGEBA/9.8 phr TETA, various test temperatures. ■ DGEBA/9.8 phr TETA, various $\dot{y}$s. ○ DGEBA/10 phr TEPE subjected to constant load prior to testing. ● DGEBA/10 phr TEPA, various $\dot{y}$s. △ DGEBA/3° amine, various $\dot{y}$s. × Rubber-modified epoxy.

stress, σ_0, by

$$K_{IB} = \sigma_0\sqrt{(\pi a)} \tag{4}$$

and the criterion for propagation of a "sharp" crack at a value of K_{Ic} may be interpreted as requiring the critical stress, σ_c, to be attained at the distance, c, such that

$$K_{Ic} = \sigma_c\sqrt{(2\pi c)}. \tag{5}$$

Thus, by rearranging Equation 3 so that

$$\frac{\sigma_0\sqrt{(\pi a)}}{\sigma_c\sqrt{(2\pi c)}} = \frac{(1+\rho/2c)^{3/2}}{(1+\rho/c)} \tag{6}$$

and substituting for Equations 4 and 5 yields

$$\frac{K_{IB}}{K_{Ic}} = \frac{(1+\rho/2c)^{3/2}}{(1+\rho/c)}. \tag{7}$$

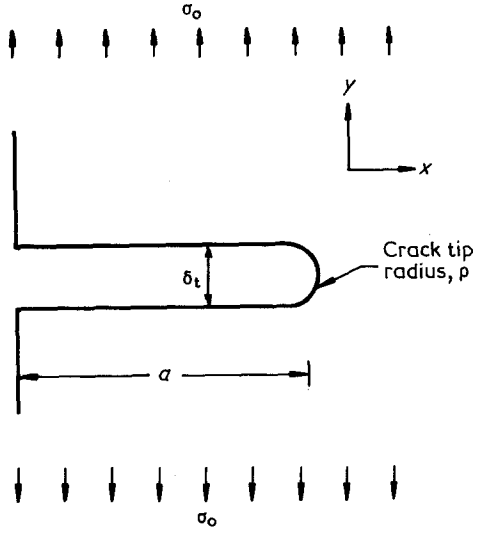

Figure 3 Crack tip geometry.

It is suggested that the crack tip radius, ρ, at failure may be taken to be directly proportional to the crack opening displacement, δ_t:

$$\rho = k\delta_t \tag{8}$$

where k is the proportionality constant. For smooth blunting, i.e. with no form of discontinuity at the tip, $k \simeq \frac{1}{2}$ and, indeed, this must form a lower bound to k. Some recent studies [17] using numerical methods would suggest that k does vary with the degree of work hardening and is about unity for a wide range of conditions.

Substituting from Equation 8 into Equation 7, we have

$$\frac{K_{IB}}{K_{Ic}} = \frac{(1+(k\delta_t)/2c)^{3/2}}{(1+(k\delta_t)/c)}. \tag{9}$$

This is not, of course, an exact solution and K_{IB} may be regarded as the elevation of K_{Ic} as a result of the δ_t arising from K_{Ic} in the original sharp tip. Using this form, we have

$$\delta_t = \frac{K_{Ic}^2}{E\sigma_y} = e_y(K_{Ic}/\sigma_y)^2 \tag{10}$$

so that on substituting into Equation 9, we have K_{IB} as a function of σ_y for a given K_{Ic}, c and e_y value. Fig. 4 shows K_{IB}/K_{Ic} as a function of $\sqrt{[(ke_y)/2c]}(K_{Ic}/\sigma_y)$ and illustrates that K_{IB}/K_{Ic} remains fairly constant, in fact decreasing slightly, until a certain value, after which it tends to the linear relationship:

$$\frac{K_{IB}}{K_{Ic}} = \frac{1}{2}\sqrt{\left(\frac{ke_y}{2c}\right)}(K_{Ic}/\sigma_y).$$

Thus, K_{IB} increases steadily with decreasing σ_y.

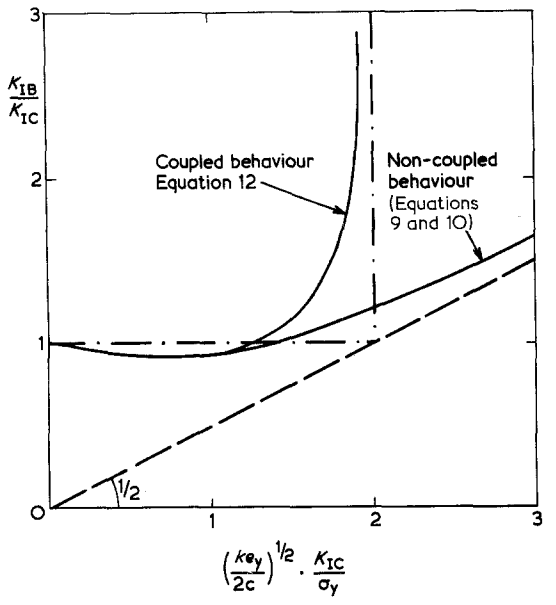

Figure 4 Theoretical curves for coupled and non-coupled blunting.

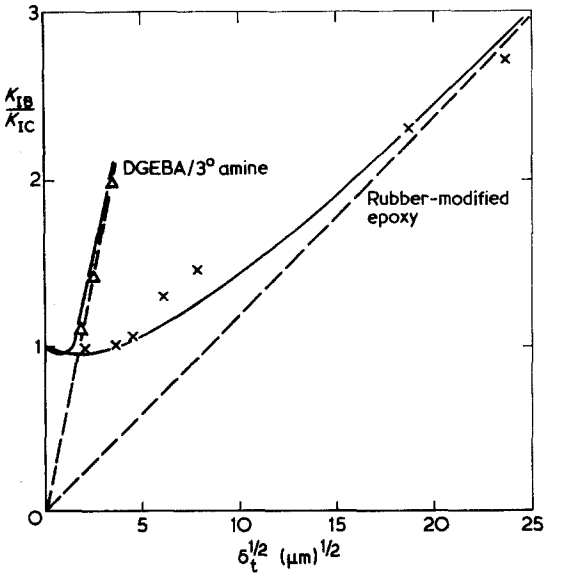

Figure 5 K_{IB}/K_{Ic} ratio versus $\delta_t^{1/2}$. Symbols as Fig. 2. Solid line – Equation 9; dashed line – approximate linear relationship from Equation 9.

Such a mechanism is probably appropriate to cases in which there is a clearly defined first stage initiating a second as, for example, in thermal blunting [18], but here we have the yield stress at the same value throughout the fracture test so that it is more sensible to write

$$\delta_t = \frac{K_{IB}^2}{E\sigma_y} = e_y(K_{IB}/\sigma_y)^2. \qquad (11)$$

Equation 9 now takes the form:

$$\frac{K_{IB}}{K_{Ic}} = \frac{\{1 + [(ke_y)/2c](K_{Ic}/\sigma_y)^2(K_{IB}/K_{Ic})^2\}^{3/2}}{\{1 + [(ke_y)/c](K_{Ic}/\sigma_y)^2(K_{IB}/K_{Ic})^2\}} \qquad (12)$$

The coupling effect of K_{IB} on δ_t gives rise to a more rapidly rising curve, as shown in Fig. 4, and for large K_{IB}/K_{Ic} we have

$$\frac{K_{IB}}{K_{Ic}} = \frac{1}{2}\sqrt{\left(\frac{ke_y}{2c}\right)\left(\frac{K_{Ic}}{\sigma_y}\right)}\,\frac{K_{IB}}{K_{Ic}}$$

so that K_{IB}/K_{Ic} tends to infinity for

$$\sqrt{\left(\frac{ke_y}{2c}\right)\left(\frac{K_{Ic}}{\sigma_y}\right)} = 2$$

and not linearity as in the non-coupled form.

An examination of the data reveals that the coupled form of relationship is much more appropriate to the data here and the results are analysed by plotting K_{IB}/K_{Ic} versus $\delta_t^{1/2}$ from Equation 11. This should tend to a linear relationship for large K_{IB} values having a slope $(1/2\sqrt{2})\sqrt{(k/c)}$.

4.2. Discussion

Values of δ_t for the epoxy materials were calculated using Equation 11 and are shown in Tables II, III and IV, and values of K_{IB}/K_{Ic} versus $\delta_t^{1/2}$ are shown in Figs. 5 and 6. The relations between K_{IB}/K_{Ic} and $\delta_t^{1/2}$ predicted by Equation 9 are

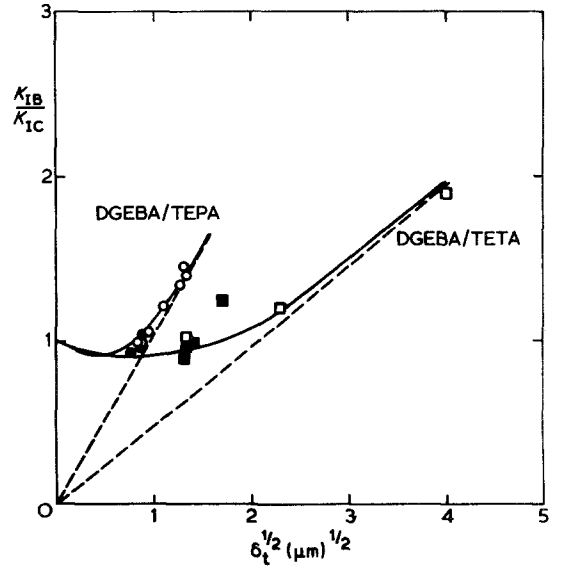

Figure 6 K_{IB}/K_{Ic} ratio versus $\delta_t^{1/2}$. Symbols as Fig. 2. Solid line – Equation 9; dashed line – approximate linear relationship from Equation 9.

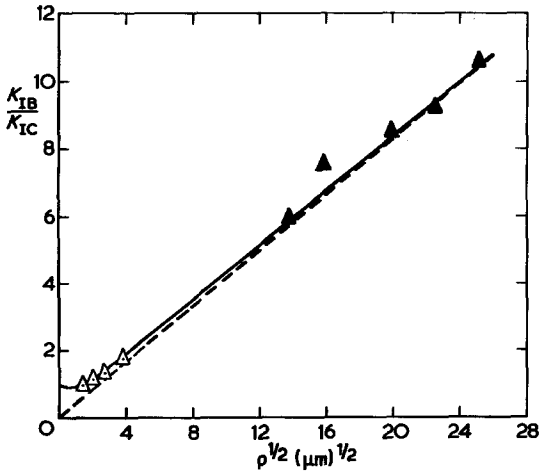

Figure 7 K_{IB}/K_{Ic} ratio versus $\rho^{1/2}$, for DGEBA/piperidine material. ▲ measured values of ρ; solid line — Equation 7, dashed line — Equation 13. △ values of ρ deduced from Equations 8 and 11 taking $k = 1$ (i.e. $\rho = \delta_t$).

indicated by the continuous solid lines and were fitted by selecting the appropriate value of k/c for each material. The experimental data and the theoretical relation from Equation 9 are in excellent agreement for all the epoxy materials. Also, the approximate linear relationships are shown dashed in Figs. 5 and 6 and are asymptotic to the relation from Equation 9 and the experimental data, as required by the above theory.

To substantiate further the above ideas and to assist in identifying the value of the proportionality constant, k, cracks of known radii were inserted into DGEBA/piperidine compact tension specimens. Blunt crack tips were formed by drilling holes at the ends of fine saw-cuts and the measured value of $\rho^{1/2}$ is plotted in Fig. 7 against the determined K_{IB}/K_{Ic} ratio. (The value of K_{Ic} was 0.73 MN m$^{-3/2}$ and was ascertained from low temperature tests on specimens containing natural cracks.) Since for these experiments ρ was measured directly Equation 7 may be fitted to the data and is shown as the solid line in Fig. 7. For $\rho \gg c$ then Equation 7 may be approximated to:

$$\frac{K_{IB}}{K_{Ic}} = \frac{1}{2}\left(\frac{\rho}{2c}\right)^{1/2} \tag{13}$$

and Equation 13 is shown as the dashed line. The value of c needed in both Equations 7 and 13 is 0.74 μm. Thus, as has been previously reported for blunt crack tests on polyvinylchloride [19], the analysis embodied in Equations 7 and 13 is in good agreement with the experimental data.

The next obvious step was to obtain a range of K_{IB}/K_{Ic} values for the DGEBA/piperidine material where self-blunting of the crack tip occurs. This data is also plotted in Fig. 7 where the value of ρ has been calculated from Equations 8 and 11 taking the value of k in Equation 8 to be unity. The experimental points are in excellent agreement with the blunt crack experimental data and with the theoretical relations. This obviously lends considerable support to the suggestion that the value of ρ is proportional to δ_t and indicates that ρ may indeed be directly equated to δ_t. This latter equality is intuitively appealing and is also in the range indicated by the analysis of McMeeking [17] and by direct measurements of ρ and δ_t of epoxy materials. This last piece of evidence was pursued by the authors by employing a small edge-cracked specimen mounted in a loading rig on the stage of an optical microscope. However, the problem of surface effects prevented accurate measurements but indicated approximately $0.5\delta_t < \rho < 2\delta_t$.

4.3. Fracture criterion

From the values of k/c required to fit Equation 9 to the experimental data, and assuming k to be $\frac{1}{2}$, 1 or 2, then corresponding values of c may be deduced for each epoxy resin. Further, from Equation 5, respective values of the critical stress, σ_c, may be calculated. Values of c and σ_c so obtained are shown in Table V.

TABLE V Values of c and σ_c for different values of k

Epoxy material	Values of k					
	$\frac{1}{2}$		1		2	
	c (μm)	σ_c (MPa)	c (μm)	σ_c (MPa)	c (μm)	σ_c (MPa)
Rubber-modified epoxy	4.2	310	8.3	220	16.6	155
DGEBA/3° amine	0.19	510	0.38	360	0.76	255
DGEBA/TETA	0.24	520	0.48	370	0.96	260
DGEBA/TEPA	0.06	700	0.12	495	0.24	350
DGEBA/piperidine	–	–	0.74	340	–	–

It may be seen from Table V that, for a given k value, the attainment of a critical stress over a critical distance provides a unique failure criterion for each material over the complete range of test conditions, irrespective of the crack growth mode. As the yield stress of the material decreases, then crack blunting becomes more severe and the lower stress concentrating effect of the blunt crack means that a higher applied stress is required to attain the value of σ_c over the distance c. The higher applied stress implies a high K_I value, i.e. $K_{IB} > K_{Ic}$, and the relatively large amount of stored elastic energy in the sample at the onset of crack propagation results in fast unstable crack growth until the energy supply is insufficient to sustain crack growth and crack arrest occurs.

The values of σ_c and c for the DGEBA/piperidine material are derived from Fig. 7 where the values of ρ come from direct measurements, as well as from calculation via Equations 8 and 11. Both methods yield values of 340 and 0.74 μm respectively. Further, as discussed above, this suggests that $k = 1$ is the appropriate value for this proportionality constant. Thus, for the epoxy materials studied values of σ_c from about 200 to 500 MPa are deduced with critical distances of about 10 to 0.1 μm respectively. The toughest materials have the lowest critical stresses but the longest critical distances. The critical stresses are of the same order as reported by Williams [20] from a fatigue model for polymethylacrylate and polycarbonate and by Ward and co-workers [21–23] who described the blunt notch fracture of these polymers using a Neuber [24] stress concentration concept. The critical stress, σ_c, may possibly be interpreted as a constrained yield stress. Such values are shown in Table V are in accord with the analysis of McMeeking [17] especially if a degree of strain hardening occurs as has been reported [3, 4] for epoxy materials.

The localized plastic deformation around the crack tip probably occurs via a shear-yielding, rather than a crazing, mechanism. Certainly for simple, well-cured epoxy materials several reviews [25, 26] have concluded that crazing does not usually occur. This has also been supported from an examination of replicas of fracture surfaces of the simple epoxy materials (molecular-weight between crosslinks about 400 [4]) using transmission electron microscopy. No evidence whatsoever was found for craze formation [13].

Thus, it seems most likely that K_{Ic}, and the associated σ_c and c values, are an alternative representation of the plane strain toughness in which the deformation is confined to a very small zone. The plastic deformation represented by σ_y is a more diffuse shear yielding which surrounds the plane strain region. It is the deformation arising from this latter region which give rise to the crack blunting which decreases the load in the plane strain region. If there is no significant blunting effect, then the plane strain behaviour dominates and controls, for example, stable growth with a constant crack-opening displacement criterion.

5. Conclusions

The circumstantial evidence for crack tip blunting as the controlling factor in the stick–slip mechanism is very strong. That this blunting is strongly influenced by the yield stress is apparent from the correlation of K_{IB} and σ_y. The model proposed here defines these interactions more precisely by describing the effect of a finite crack tip radius on toughness and then relates this radius to crack opening displacement. The model works well and gives parameters defining the fracture strength which will require further investigation. The exact nature of the plane strain toughness and the associated shear yield behaviour is also not completely clear and would be much helped by direct observations.

Acknowledgements

The authors would like to thank Dr R. J. Young (Queen Mary College), Mr S. J. Shaw (PERME) and Dr D. Tod (PERME) for many useful discussions and comments during the course of this work. This paper is printed with the kind permission of the Controller, HMSO.

References

1. J. F. KNOTT, "Fundamentals of Fracture Mechanics" (Butterworths, London, 1973).
2. J. G. WILLIAMS, "Stress Analysis of Polymers" (Longmans, London, 1973).
3. R. A. GLEDHILL, A. J. KINLOCH, S. YAMINI and R. J. YOUNG, *Polymer* **19** (1978) 574.
4. R. A. GLEDHILL and A. J. KINLOCH, *Polymer Eng. Sci.* **19** (1979) 82.
5. S. MOSTOVOY, E. J. RIPLING and C. F. BERSCH, *J. Adhesion* **3** (1971) 125.
6. S. YAMINI and R. J. YOUNG, *Polymer* **18** (1977) 1075.
7. R. A. GLEDHILL and A. J. KINLOCH, *J. Mater. Sci.* **10** (1975) 1261.
8. D. C. PHILLIPS and J. M. SCOTT, *ibid.* **9** (1974)

1202.
9. K. SELBY and L. E. MILLER, *ibid.* **10** (1975) 12.
10. R. J. YOUNG and P. W. R. BEAUMONT, *ibid.* **10** (1975) 1343.
11. E. J. RIPLING, S. MOSTOVOY and C. BERSCH, *J. Adhesion* **3** (1971) 145.
12. R. A. GLEDHILL, A. J. KINLOCH and S. J. SHAW, *J. Mater. Sci.* **14** (1979) 1769.
13. A. J. KINLOCH and S. J. SHAW, International Conference on Adhesion and Adhesives, Durham September (1980).
14. M. I. HAKEEM and M. G. PHILLIPS, *J. Mater. Sci.* **13** (1978) 2284.
15. B. W. CHERRY and K. W. THOMSON, *Int. J. Fracture* **14** (1978) R17.
16. J. M. SCOTT, D. C. PHILLIPS and M. JONES, *J. Mater. Sci.* **13** (1978) 311.
17. R. M. McMEEKING, *J. Mech. Phys. Solids* **25** (1977) 357.
18. J. G. WILLIAMS and J. M. HODGINKINSON, to be published.
19. I. CONSTABLE, L. E. CULVER and J. G. WILLIAMS, *Int. J. Fracture Mech.* **6** (1970) 279.
20. J. G. WILLIAMS, *J. Mater. Sci.* **12** (1977) 2525.
21. R. A. W. FRASER and I. M. WARD, *ibid.* **9** (1974) 1624.
22. *Idem, ibid.* **12** (1977) 459.
23. G. L. PITMAN, I. M. WARD and R. A. DUCKETT, *ibid.* **13** (1978) 2092.
24. H. NEUBER, "Theory of Notch Stresses" (Julius Springer, Berlin, 1937).
25. R. J. YOUNG, in "Development in Polymer Fracture-1", edited by E. H. Andrews (Applied Science, London, 1979) p. 183.
26. A. J. KINLOCH, *Metal Sci.* **14** (1980) to be published.

Received 7 August and accepted 20 September 1979.